We are IntechOpen,
the world's leading publisher of
Open Access books
Built by scientists, for scientists

6,900
Open access books available

186,000
International authors and editors

200M
Downloads

154
Countries delivered to

Our authors are among the

TOP 1%
most cited scientists

12.2%
Contributors from top 500 universities

BOOK CITATION INDEX
CLARIVATE ANALYTICS
INDEXED

WEB OF SCIENCE™

Selection of our books indexed in the Book Citation Index
in Web of Science™ Core Collection (BKCI)

Interested in publishing with us?
Contact book.department@intechopen.com

Numbers displayed above are based on latest data collected.
For more information visit www.intechopen.com

Chapter

Computational Studies of Drug Repurposing Targeting P-Glycoprotein-Mediated Multidrug-Resistance Phenotypes in Agents of Neglected Tropical Diseases

Nivedita Jaishankar, Sangeetha Muthamilselvan and Ashok Palaniappan

Abstract

Mammalian ABCB1 P-glycoprotein is an ATP- dependent efflux pump with broad substrate specificity associated with cellular drug resistance. Homologous to this role in mammalian biology, the P-glycoprotein of agents of neglected tropical diseases (NTDs) mediates the emergence of multidrug-resistance phenotypes. The clinical and socioeconomic implications of NTDs are exacerbated by the lack of research interest among Big Pharma for treating such conditions. This work aims to characterise P-gp homologues in certain agents of key NTDs, namely (1) Protozoa: *Leishmania major, Trypanosoma cruzi*; (2) Helminths: *Onchocerca volvulus, Schistosoma mansoni*. Based on structural modelling of the organismal P-gp homologues, potential antibiotics targeting these structures were identified based on similarity and repurposing of existing drugs. Docking studies of the Pgp receptor—antibiotic ligand complexes were carried out and the most tenable target-ligand conformations assessed. The interacting residues were identified, and binding pockets studied. The in silico studies yielded measurements of the relative efficacy of the new drugs, which need experimental validation. Our studies could lay the foundation for the development of effective synergistic or new therapies against key neglected tropical diseases. The potential mechanisms of multidrug resistance emergence in *E. coli* were examined.

Keywords: P-glycoprotein, neglected tropical diseases, multidrug resistance, homology modeling, receptor-ligand docking, differential ligand affinity, synergistic effects, leishmaniasis, trypanosomiasis, onchocerciasis, schistosomiasis

1. Introduction

1.1 Multidrug resistance (MDR)

Bacterial evolution has been constrained to respond to the selection pressure of antibiotics and combined with their reckless use and has led to the emergence of varied defenses against antimicrobial agents. The main mechanisms whereby the bacteria develop resistance to antimicrobial agents include enzymatic inactivation, modification of the drug target(s), and reduction of intracellular drug concentration by changes in membrane permeability or by the over expression of efflux pumps [1]. Multidrug resistance efflux pumps are recognized as an important component of resistance in both Gram-positive and Gram-negative bacteria [2]. Some bacterial efflux pumps may be selective for one substrate or transport antibiotics of different classes, conferring a multiple drug resistance (MDR) phenotype. With respect to efflux pumps, they provide a self-defense mechanism whereby antibiotics are extruded from the cell interior to the external environment. This results in sublethal drug concentrations at the active site that in turn may predispose the organism to the development of high-level target-based resistance [3]. Therefore, efflux pumps are viable antibacterial targets, and identification and development of potent efflux pump inhibitors is a promising and valid strategy potential therapeutic agents that can rejuvenate the activity of antibiotics that are no longer effective against bacterial pathogens. The world is searching for new tools to combat multidrug resistance.

1.2 P-glycoprotein

P-glycoprotein is a mammalian multidrug-resistance protein belonging to the ATP-binding cassette (ABC) superfamily [4]. It is an ATP-dependent efflux pump encoded by the MDR1 gene and is primarily found in epithelial cells lining the colon, small intestine, pancreatic ductules, bile ductules, kidney proximal tubes, the adrenal gland, and the blood-testis and the blood-brain barrier [5]. This efflux activity of P-glycoprotein, coupled with its wide substrate specificity, is responsible for the reduction in bioavailability of drugs as it extrudes all foreign substances such as drugs and xenobiotics out of the cells. ATP hydrolysis provides energy for the efflux of drugs from the inner leaflet of the cell membrane [6, 7]. This protein is believed to have evolved as a defense mechanism against toxic compounds and prevent their entry into the cytosol [8].

P-glycoprotein confers resistance to a wide range of structurally and functionally diverse compounds, which has resulted in the emergence of multidrug resistance in medically relevant microorganisms. The pharmacodynamic role of P-glycoprotein in parasitic helminths has widespread clinical and socioeconomic implications, exacerbating the problem of neglected tropical diseases (NTDs) whose causative agents are helminths and protozoa.

Sheps et al. [9] reported that 15 P-glycoproteins are present in *Caenorhabditis elegans*, and Laing et al. [10] reported that 10 homologous P-glycoproteins were present in *Haemonchus contortus*. A bioinformatic and phylogenetic study conducted by Bourguinat et al. [11] on the *Dirofilaria immitis* genome identified three orthologous ABC-B transporter genes. These genes are suspected to be responsible for the P-glycoprotein-mediated drug extrusion of melarsomine in *D. immitus* and other parasites.

1.3 Neglected tropical diseases

Neglected tropical diseases (NTDs) encompass 17 bacterial, parasitic, and viral diseases that prevail in tropical and subtropical conditions in 149 countries and affect more than 1 billion people worldwide, according to WHO.

1.3.1 Leishmaniasis

Leishmaniasis is a disease caused by parasites of the Leishmania type. It is spread by the bite of certain types of sandflies [12]. The disease can present in three main ways: cutaneous, mucocutaneous, or visceral leishmaniasis [13]. The cutaneous form presents with skin ulcers, whereas the mucocutaneous form presents with ulcers of the skin, mouth, and nose [12]. Leishmaniasis is transmitted by the bite of infected female phlebotomine sand flies [14] which can transmit the protozoa *Leishmania*.

Gammaro et al. [12] first reported that the overexpression of P-glycoprotein in *Leishmania* species was responsible for the drug resistance of the organisms against drugs such as methotrexate. The multidrug resistance has been associated with several ATP-binding cassette transporters including MRP1 (ABCC1) and P-glycoprotein (ABCB1). Wyllie et al. [15] demonstrated the presence of metal efflux pumps in the cell membrane of all *Leishmania* species. Soares et al. [16] reported that natural or synthetic modulators of human P-glycoprotein such as flavonoids restore sensitivity to pentamidine, sodium stibogluconate, and miltefosine by modulating intracellular drug concentrations.

1.3.2 Onchocerciasis

Onchocerciasis, also known as river blindness, is a disease caused by infection with the parasitic worm *Onchocerca volvulus* and is transmitted by the bite of an infected black fly of the *Simulium* type. Symptoms include severe itching, bumps under the skin, and blindness. It is the second most common cause of blindness due to infection, after trachoma, according to WHO. Usually, many bites are required before infection occurs. A vaccine against the disease does not exist. Prevention is by avoiding being bitten by flies.

Ivermectin (IVM) is a semisynthesized macrocyclic lactone that belongs to the avermectin class of compounds. It is administered en masse and but is effective only against microfilariae [17]. Bourguinat et al. [11] have found evidence of IVM resistance in *Onchocerca volvulus*. The clinical trial sampled patients before and after IVM treatment over a period of 3 years. The nodules collected from the patients contained IVM-resistant *O. volvulus* worms.

1.3.3 Schistosomiasis

Schistosomiasis is a disease caused by infection with one of the species of *Schistosoma* helminthic flatworms known as flukes belonging to the class Trematoda of the phylum Platyhelminthes. There are three main species of *Schistosoma* associated with human disease: *Schistosoma mansoni* and *Schistosoma japonicum* cause intestinal schistosomiasis, and *Schistosoma haematobium* causes genitourinary schistosomiasis. Other *Schistosoma* species have been recognized less commonly as agents of intestinal schistosomiasis in humans [18]. Pinto-Almeida et al. [19] demonstrated that drug resistance by *Schistosoma mansoni* to praziquantel (commonly employed drug) is mediated by efflux pump proteins, including P-glycoprotein and multidrug resistance-associated proteins.

1.3.4 Trypanosomiasis

The trypanosomiasis consists of a group of diseases caused by parasitic protozoa of the genus *Trypanosoma*. There are two main parasites such as *Trypanosoma brucei*, which causes the sleeping sickness or human African trypanosomiasis and *Trypanosoma cruzi*, which causes the Chagas' disease or American trypanosomiasis

[20]. These diseases are transmitted by several arthropod vectors such as *Glossina* and *Triatominae*. Chaga's disease causes 21,000 deaths per year mainly in Latin America [21]. Benznidazole and Nifurtimox, only available drugs, however, have limited efficacy in the advanced stages of the disease [22]. Liu et al. [23] and Rappa et al. [24] concluded that *Trypanosoma cruzi* develops resistance to the drugs after prolonged treatment. It was shown that this happens due to the overexpression of the MDR1 gene, at high levels of the drug, which accumulates in the cells over time. Campos et al. [25] demonstrated that the drug resistance is continued throughout the life cycle of the worm.

2. Methods

The methodology is essentially similar to that in our earlier study on P-glycoproteins in priority infectious agents [26].

2.1 Determining the full helminthic complement of efflux pump proteins homologous to mammalian P-glycoprotein

The protein sequence of the human P-glycoprotein (P08183) was obtained from the SWISS-PROT database. The position-specific iterated BLAST (PSI-BLAST) was performed against a search set of nonredundant protein sequences in the organism of interest, using hPGP as the query. Through a PSI-BLAST search, a large set of related proteins are compiled. It is used to identify distant evolutionary relationships between protein sequences [27]. In the algorithm, parameters were set with an E-value of 0.001, and the scoring matrix BLOSUM62 was used. This step was performed on all four organisms of interest (*Leishmania major*, *Onchocerca volvulus*, *Schistosoma mansoni*, and *Trypanosoma cruzi*). Hundreds of hits were obtained for P-glycoprotein, and these results were prioritized according to predetermined parameters such as medical relevance, annotation status, and the presence of conserved regions. Sequences having a high percentage of sequence identity and query coverage were prioritized. Specific UniProt searches of these protein sequences were performed using the accession number. The results were analyzed, and the P-glycoprotein sequence of each organism was finalized.

2.2 Multiple sequence alignment

The templates chosen for multiple sequence alignment (MSA) were 4M1M (*Mus musculus*), 4F4C (*Caenorhabditis elegans*), 3WME (*Cyanidioschyzon merolae*), 2HYD (*Staphylococcus aureus*), 3B5Z (*Salmonella enterica*). These five metazoan, algal, and bacterial templates were used due to their high sequence identity with the hPGP sequence. The target sequences and the five templates were aligned using ClustalX 2.1 [28]. MSA was performed in order to infer the homology and evolutionary relationship between the sequences of the biological data set. The clustering algorithm used was Neighbor Joining (NJ). The phylogenetic distance between the target sequence and the templates was calculated.

2.3 Homology modeling

The chosen P-glycoprotein sequences were used as target sequences for modeling using software such as SWISS-MODEL. SWISS-MODEL is an open-source, structural bioinformatics tool used for the automated comparative modeling of three-dimensional protein structures [29, 30]. Several P-glycoprotein structures

were modeled for each organism, using multiple templates. The templates having high sequence similarity with the target sequences were given preference. The models were built, and the PDB files of the structures were obtained.

2.4 Structure validation

The validity of the structures was checked using Procheck, an open source tool used to assess the reliability of the protein structure. It is a part of the SWISS-MODEL server. The structures were refined using energy-minimization protocols, and the least energetic structure corresponding to each protein was chosen for docking studies. The criteria used to assess the quality of the structure include model geometry and the Ramachandran plot. The Ramachandran plot describes the rotation of the polypeptide backbone around the N-C_α (ϕ) and C-C_α (ψ) bonds. It provides an overview of the distribution of the torsion angles over the core, allowed, generous, and disallowed regions. The three main parameters used to select the structures were:

1. Overall Ramachandran value

2. Phylogenetic tree distance

3. Taxonomy

2.5 Creation of the ligand dataset

The ligand data set was created by surveying the literature to determine the drugs which the pathogenic helminths are both sensitive and resistant to. Drug resistance which was conferred via efflux pump activity was given importance. This set of ligands was created for each efflux pump, comprising known and potential antibiotics. The canonical *simplified molecular-input line-entry system* (SMILES) of each drug was retrieved from the PubChem database. The PDB model of each antibiotic was then generated using MarvinView by converting the canonical SMILES [31].

2.6 Protein and ligand preparation

The efflux pump proteins and ligands were individually docked using the AutoDock Version 4.2.6 suite of programs [32]. The software consists of two main programs: AutoGrid, which precalculates a set of grid points on the receptor, and AutoDock, which docks the ligand to the receptor through the grids. The PDB files of the P-glycoprotein structures and the ligands were modified through the addition of Gasteiger charges, followed by the addition and merging of hydrogen atoms to each structure. These modified structures were then saved as PDBQT files using the AutoDock tools. A uniform grid box was then defined and centered in the internal binding cavity of each P-glycoprotein structure, and the affinity maps were generated using AutoGrid. This procedure was repeated for each protein-drug complex.

2.7 Molecular docking of the helminthic efflux pumps with known and potential antibiotics

Each drug was individually docked with each target protein using AutoDock 4.2.6. The local search algorithm used was the Lamarckian genetic algorithm, set to its default parameters. The docking parameters were set to 250,000 cycles per run

and 10 runs per protein-drug complex, to obtain the 10 best poses for each complex. The best pose was defined as the conformation having the least binding energy. The 10 poses obtained for each receptor-ligand pair were clustered at 2.0 Å r.m.s. to validate the convergence to the best pose. The AutoDock was run, and the PDBQT file of the best pose of each docked complex was generated.

The results were analyzed to verify whether the pathogenic strain could develop resistance to known antibiotics using efflux pump activity and if the novel antibiotics could be effective against the development of such resistance.

2.8 Calculation of differential ligand binding affinity

The differential binding affinities of the repurposed ligands were determined using the conventionally used drugs as a baseline. A lower value is indicative of a more stable complex. The differential affinity of the potential drug for a given efflux pump protein relative to the known drug is estimated as the difference in the binding energies of the known and potential drugs, as given by Eq. (1):

$$\Delta\Delta G_{invest.known} = \Delta G_{bind,potential} - \Delta G_{bind,known} \tag{1}$$

where $\Delta\Delta G_{invest.known}$ = differential ligand affinity, kcal/mol; ΔG_{bind} = free energy of binding, kcal/mol.

2.9 Identification of interacting residues in each docked complex

The best pose of each docked complex was viewed using RasMol [33], and all interacting residues within a radius of 4.5 Å of the ligand were selected. The PDBQT file of each restricted complex was saved as a PDB file. The interacting residues of each docked complex were then analyzed.

3. Results and discussion

Extensive literature searches on Neglected Tropical Diseases (NTDs) showed that leishmaniasis, onchocerciasis, schistosomiasis, and trypanosomiasis have started exhibiting multidrug resistance, mediated by P-glycoprotein efflux pumps [11, 12, 25, 34]. New drugs targeting NTD's are undergoing clinical trials [35–37], and efforts are being taken to uncover the mechanisms of drug resistance employed by the causative helminths.

The sequence identity of each helminthic P-glycoprotein with the human P-glycoprotein (hPGP) which was retrieved from the UniProt database (UniProt ID: P08183) was determined by running a PSI-BLAST.

3.1 Psi-blast analysis

The PSI-BLAST was performed on each target organism using hPGP as the query. The results were refined according to predetermined parameters such as medical relevance, annotation status, and the presence of conserved regions. The chosen efflux pump protein sequences were shown in **Table 1**.

The top hits of each PSI-BLAST were analyzed, and the hit having the highest Max Score was chosen only in the case of *Leishmania major* and *Onchocerca volvulus*. These protein sequences were fully annotated and had high sequence identities over a large portion of the protein sequence. The top hits of the PSI-BLAST of *Schistosoma mansoni* and *Trypanosoma cruzi* with hPGP yielded results having high

Organism	Name of protein	Sequence length	% of identity	Query coverage	Max score
Leishmania major	P-glycoprotein	1341	36%	98%	767
Onchocerca volvulus	P-glycoprotein	1278	37%	97%	776
Schistosoma mansoni	SMDR2	1254	40%	98%	889
Trypanosoma cruzi	P-glycoprotein	1034	29%	30%	79.7

Table 1.
PSI-BLAST results of the target organisms using hPGP as the query.

Max Scores, but low query coverage. These protein sequences were also found to be unannotated. For these reasons, the proteins which had a lower Max Score in comparison to other results, but satisfied other parameters, were chosen.

3.2 Template selection and multiple sequence alignment

Certain metazoan, algal and bacterial crystal structures shown in **Table 2** were selected as potential templates for homology modeling [38].

Each target protein sequence was aligned with the set of chosen templates using ClustalX 2.1. The MSA between Leishmania major and the 4M1M and 4F4C templates showed the highest sequence identity, as shown in **Figure 1**. Additionally, the phylogenetic distances between the sequences were calculated using the NJ algorithm (**Table 3**).

3.3 Homology modeling

The chosen P-glycoprotein sequences of the organisms were used as target sequences for homology modeling using the SWISS-MODELER. Each protein was modeled using several templates, and the predetermined templates were used if they were found to have a fairly high GMQE score. Each modeled structure was saved as a PDB file. The results are summarized in **Table 4**.

Global Model Quality Estimation (GMQE) is a score that provides an estimation of the quality of the alignment. It is expressed as a value between 0 and 1, where the reliability of the model is directly proportional to the score. The GMQE of the homology models are found to be (mostly) between 0.60 and 0.70 for all organisms, with the exception of *Trypanosoma cruzi*, which gave scores in the range 0.29–0.52.

The templates 4M1M, 4F4C, and 3WME were found to be comparatively more reliable. Hence, only the protein structures modeled using these templates were used for further validation studies.

Template	Organism
4M1M	*Mus musculus*
4F4C	*Canorhabditis elegans*
3WME	*Cyanidioschyzon merolae*
2HYD	*Staphylococcus aureus*
3B5Z	*Salmonella enteric*

Table 2.
Templates chosen for multiple sequence alignment.
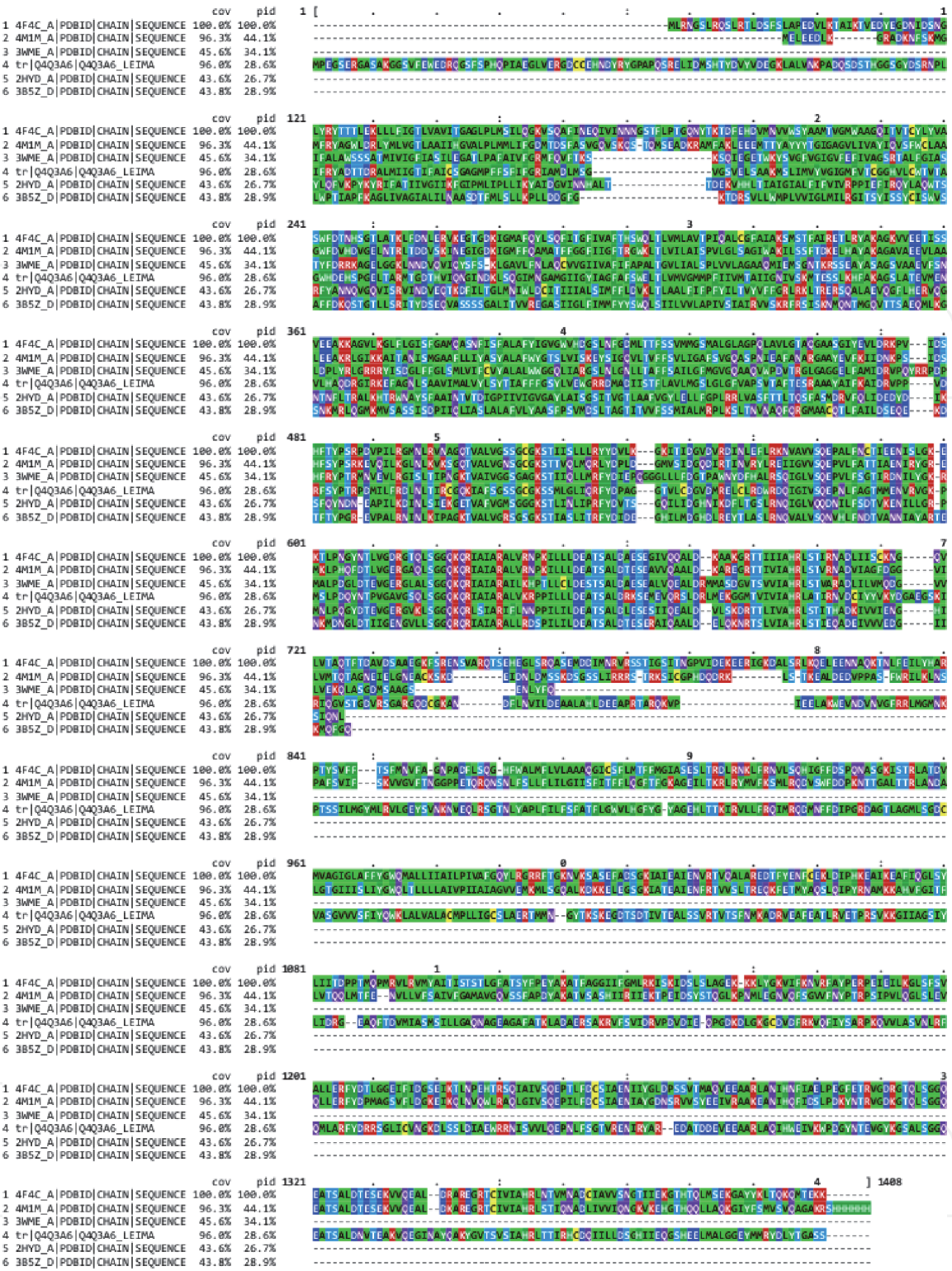
Figure 1.
Multiple sequence alignment of the target sequence P-glycoprotein of Leishmania major *(tr_Q4Q3A6) with the templates of interest.*

3.4 Structure validation

The quality of each structure was assessed using Procheck. Criteria such as model geometry and the Ramachandran plot were used to validate the structures. The PDB file of each structure was used to run the Procheck, and the Ramachandran plot values were obtained. The Ramachandran values are summarized in **Table 5**.

Template	Phylogenetic distance			
	Leishmania major	*Onchocerca volvulus*	*Schistosoma mansoni*	*Trypanosoma cruzi*
4M1M	0.685	0.648	0.646	**0.847**[*]
4F4C	**0.642**	**0.638**	**0.605**	0.861
3WME	0.653	0.679	0.649	0.867
2HYD	0.72	0.709	0.694	0.826
3B5Z	0.731	0.707	0.698	0.841

[*]*The distance between* T. cruzi *and 4M1M is prioritized as the 4M1M and 4F4C templates were found to have higher sequence identity with the helminthic P-glycoproteins.*
Bold values signify the final template in the case of each agent.

Table 3.
Phylogenetic distance matrix between the target sequence of each organism and the templates.

Organism	Template	Sequence identity	Query coverage	GMQE
Leishmania major	4F4C	34.43	0.91	0.64
	4M1M	36.09	0.90	0.65
	3WME	37.30	0.43	0.29
	4Q9I	36.20	0.90	0.65
	4KSC	38.25	0.90	0.64
	4KSB	38.25	0.90	0.64
	5KPJ	38.25	0.90	0.66
Onchocerca volvulus	4F4C	38.83	0.97	0.69
	4M1M	37.10	0.96	0.69
	3WME	31.75	0.44	0.33
	3G5U	38.77	0.95	0.66
	4KSB	38.77	0.95	0.67
	4Q9I	36.97	0.95	0.69
	4LSG	38.77	0.95	0.67
Schistosoma mansoni	4F4C	38.60	0.97	0.69
	4M1M	36.09	0.90	0.65
	3G5U	39.41	0.97	0.68
	3G60	42.11	0.95	0.68
	5KPJ	39.52	0.97	0.70
	4KSC	42.11	0.95	0.69
	4KSB	42.11	0.95	0.69
	4LSG	39.41	0.97	0.69
Trypanosoma cruzi	4F4C	15.11	0.81	0.45
	4M1M	14.36	0.78	0.29
	3WME	18.37	0.51	0.33
	4KSC	14.23	0.79	0.44
	3G5U	14.46	0.78	0.43
	5TSI	23.43	0.90	0.52
	4LSG	14.46	0.78	0.43

Table 4.
Homology modeling results.

The structures were finalized by analyzing overall Ramachandran value, Phylogenetic tree distance, and taxonomy parameters. The 4F4C template was found to suitable for all the organisms excluding *Leishmania major*, for which the 4M1M template was selected (**Table 5**).

3.4.1 Validation of the P-glycoprotein structure modeled using the 4M1M template for Leishmania major

The Ramachandran plots having a core region of at least 90% are prioritized for further studies. The core, allowed, generous and disallowed regions are colored and distinguished (**Figure 2**). The red, brown, and yellow regions represent the favored, allowed, and generously allowed regions.

A more comprehensive analysis of the structure is provided by other programs that generate other data such as Phi-Psi graphs and Chi1-Chi2 plots for each residue type. Each Phi-Psi plot provides an analysis of the torsion angle of each residue type. The red, brown, and yellow regions represent the favored, allowed, and generously allowed regions (shown in **Figure 3**).

The Chi1-Chi2 plot describes the side-chain torsion angles combinations for each amino acid [28]. The darker regions indicate a more favorable angle combination (shown **Figure 4**).

3.4.2 Validation of the P-glycoprotein structure modeled using the 4F4C template for Onchocerca volvulus, Schistosoma mansoni and Trypansoma cruzi

For all the three P-glycoproteins, the structures were modeled using the 4F4C template and as such and showed remarkable structural similarity with respect to the Ramachandran plot (90.8% in the core region), and residue torsion angles. **Figures 5**–**7** summarize this exercise.

3.5 Creation of the ligand dataset

Upon extensive survey of the literature, a comprehensive data set of the known and potential drugs was compiled (**Table 6**). The list of potential drugs comprises of both unapproved, investigational drugs that are undergoing phase trials, and FDA approved antibiotics. In this study, these known drugs have been repurposed for other helminthic diseases.

3.6 Molecular docking of the helminthic efflux pumps with known and potential antibiotics

The molecular docking was carried out using the AutoDock suite of tools. The search algorithm used was the Lamarckian Genetic Algorithm, and the docking parameters were set to 10 runs per protein-drug complex. Each docked complex yielded 10 poses, and the best pose was defined as the conformation possessing the least free binding energy.

3.6.1 Molecular docking results of benznidazole with P-glycoprotein (Leishmania major)

The drug benznidazole is docked with P-glycoprotein (*Leishmania major*), and their interaction is studied (**Table 7**). The best pose has a free binding energy of −5.00 kcal/mol. The clustering was performed at 2.0 Å r.m.s. to validate the convergence to the best pose. The clustering figure (**Figure 8**) shows closer peaks near −2.5 kcal/mol, whereas the least binding energy of the complex, that is, most

			Leishmania major					
Template	Core region	Additionally allowed region	Generously allowed region	Disallowed region	No. of residues	Query coverage	Sequence identity	Phylogenetic distance
4F4C	90.8	8.1	1.2	0	1250	0.43	34.43	0.685
4M1M	92	6.4	1.4	0.2	1188	0.9	36.09	0.642
3WME	94.6	4.6	0.4	0.4	573	0.43	36.46	0.653
			Onchocerca volvulus					
Template	Core region	Additionally allowed region	Generously allowed region	Disallowed region	No. of residues	Query coverage	Sequence identity	Phylogenetic distance
4F4C	90.8	8.1	1.2	0	1250	0.97	38.83	0.648
4M1M	91.1	7.6	1.2	0.1	571	0.95	37.1	0.638
3WME	93.1	5.8	0.6	0.6	1180	0.45	33.51	0.679
			Schistosoma mansoni					
Template	Core region	Additionally allowed region	Generously allowed region	Disallowed region	No. of residues	Query coverage	Sequence identity	Phylogenetic distance
4F4C	90.8	8.1	1.2	0	1250	0.97	38.6	0.646
4M1M	91.1	6.9	1.8	0.2	572	0.46	36.6	0.605
3WME	93.7	5.8	0.2	0.4	567	0.45	38.31	0.649
			Trypanosoma cruzi					
Template	Core region	Additionally allowed region	Generously allowed region	Disallowed region	No. of residues	Query coverage	Sequence identity	Phylogenetic distance
4F4C	90.8	8.1	1.2	0	1250	0.81	15.11	0.847
4M1M	86.0	11.9	1.8	0.2	1034	0.51	17.80	0.867
3WME	89.8	8	1.6	0.6	573	0.51	18.37	0.861

Table 5.
Justification of the template chosen for each organism using the Ramachandran plot values and the phylogenetic distance between the target protein and the template.
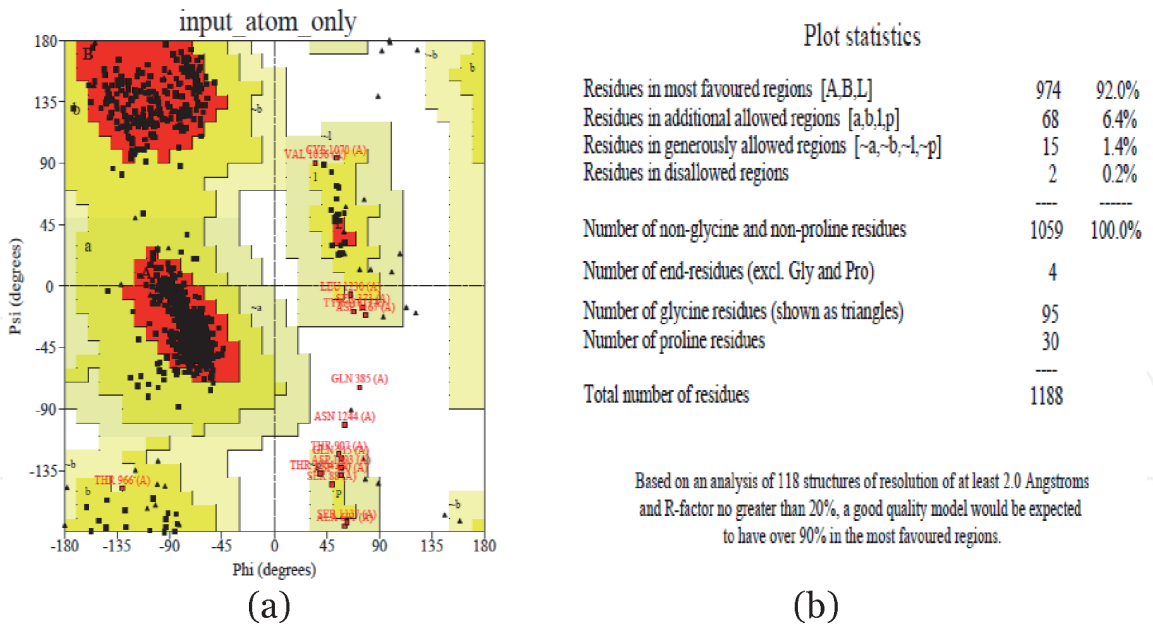
Figure 2.
(a) The Ramachandran plot generated for P-glycoprotein (Leishmania major), modeled using the 4M1M template and (b) plot statistics of the P-glycoprotein (Leishmania major), modeled using the 4M1M template.
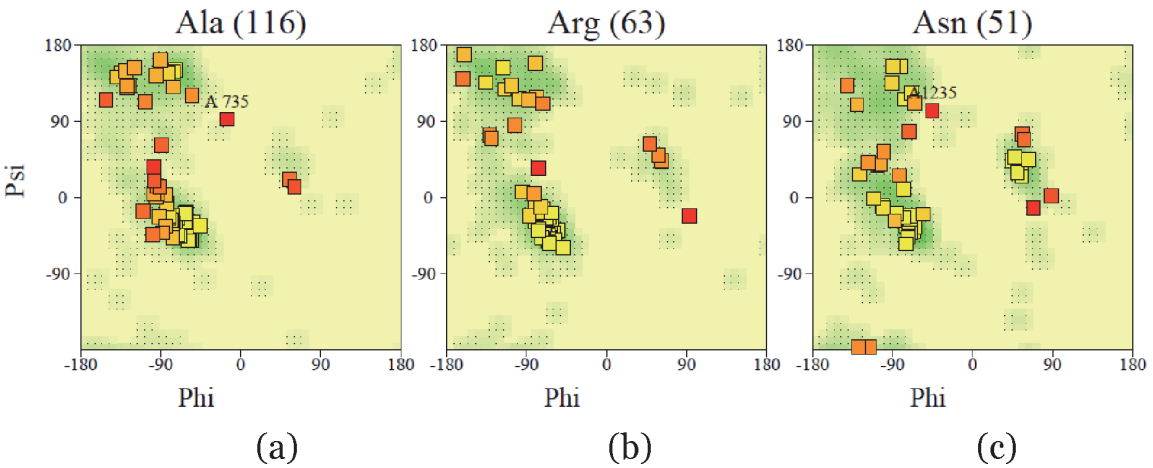
Figure 3.
Phi-psi plot of residues of the P-glycoprotein structure of Leishmania major, *modeled using the 4M1M template (a) Ala, (b) Arg, and (c) Asn.*
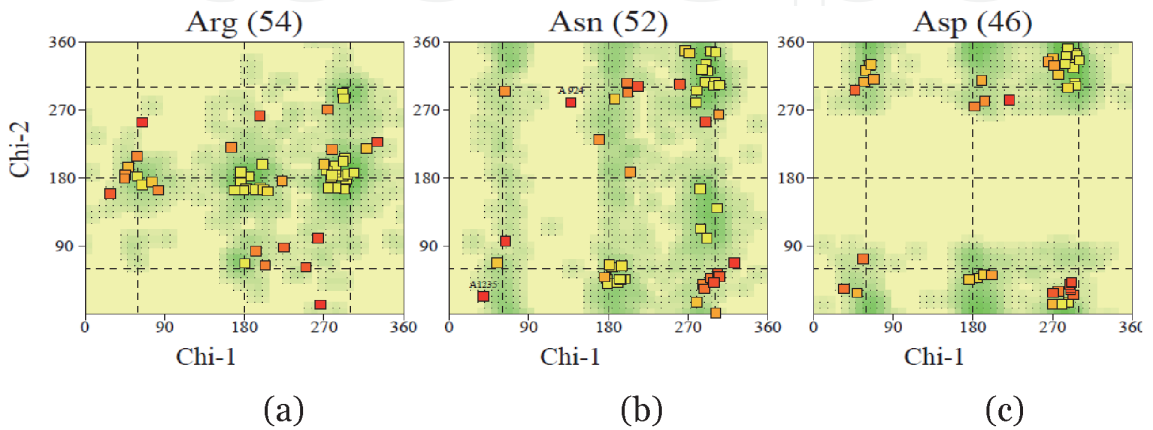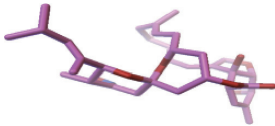

Figure 4.
Chi1-Chi2 plot of residues of the P-glycoprotein structure of Leishmania major, *modeled using the 4M1M template (a) Arg, (b) Asn and (c) Asp.*
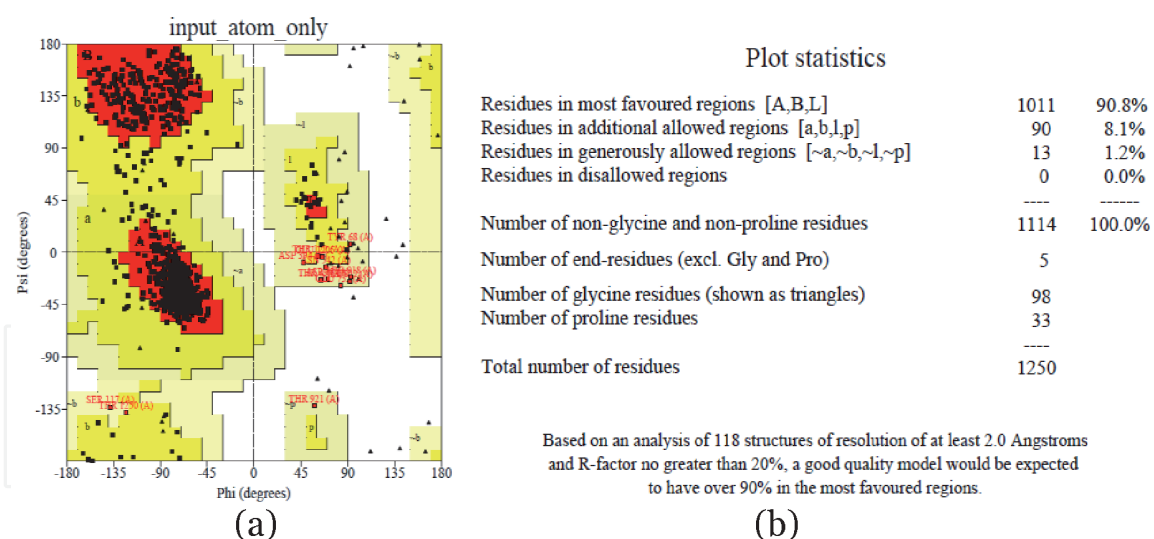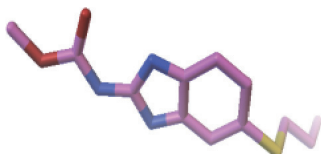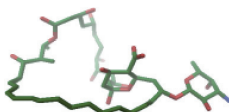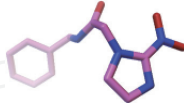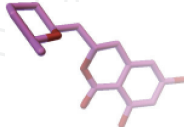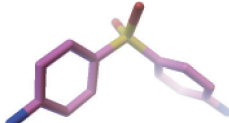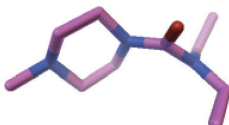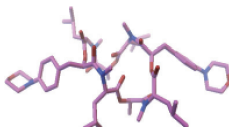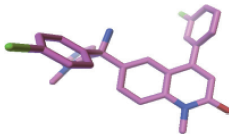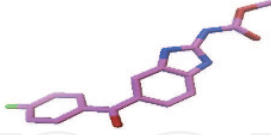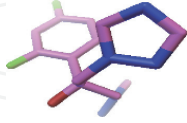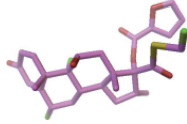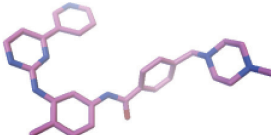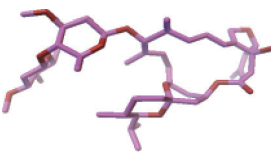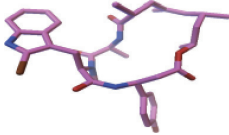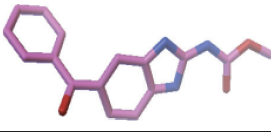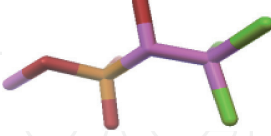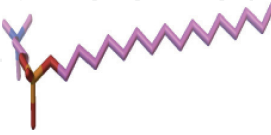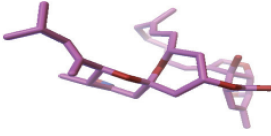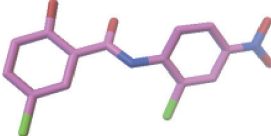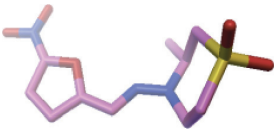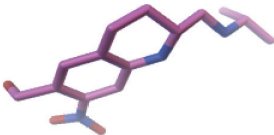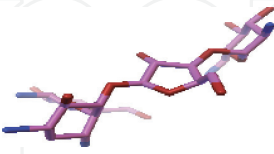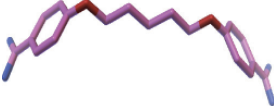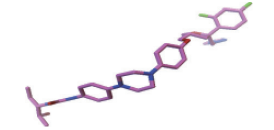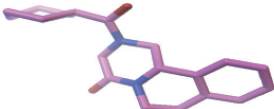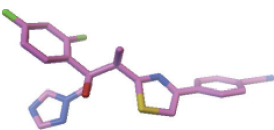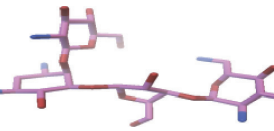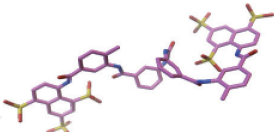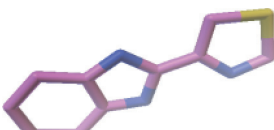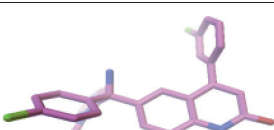
Figure 5.
(a) The Ramachandran plot generated for P-glycoprotein (Onchocerca volvulus), modeled using the 4F4C template and (b) plot statistics of the P-glycoprotein (Onchocerca volvulus), modeled using the 4F4C template.

S. no.	Drug	PubChem CID	3-D Structure
1.	Albendazole	2082	
2.	Amphotericin B	5280965	
3.	Artesunate	65664	
4.	Benznidazole	5798	
5.	Cladosporin	13990016	
6.	Dapsone	2955	
7.	Diethylcarbamazine	15432	
8.	Emodepside	6918632	

13

S. no.	Drug	PubChem CID	3-D Structure
9.	Fexinidazole	68792	
10.	Flubendazole	35802	
11.	Fluconazole	3365	
12.	Furozan	67517	
13.	Imatinib	5291	
14.	Ivermectin	6321424	
15.	Jaspamide	9831636	
16.	Mebendazole	4030	
17.	Metrifonate	5853	
18.	Miltefosine	3599	
19.	Moxidectin	9832912	
20.	Niclosamide	4477	

S. no.	Drug	PubChem CID	3-D Structure
21.	Nifurtimox	6842999	
22.	Oxamniquine	4612	
23.	Paromomycin	165580	
24.	Pentamidine	4735	
25.	Posaconazole	468595	
26.	Praziquantel	4891	
27.	Ravuconazole	467825	
28.	Sodium stibogluconate	76968133	
29.	Suramin	5361	
30.	Terbinafine	1549008	
31.	Thiabendazole	5430	
32.	Tipifarnib	159324	

3D structures of the drugs are visualized using python molecular viewer (PMV-1.5.6).

Table 6.
PubChem compound ID and 3D structure of the ligands used for docking studies.
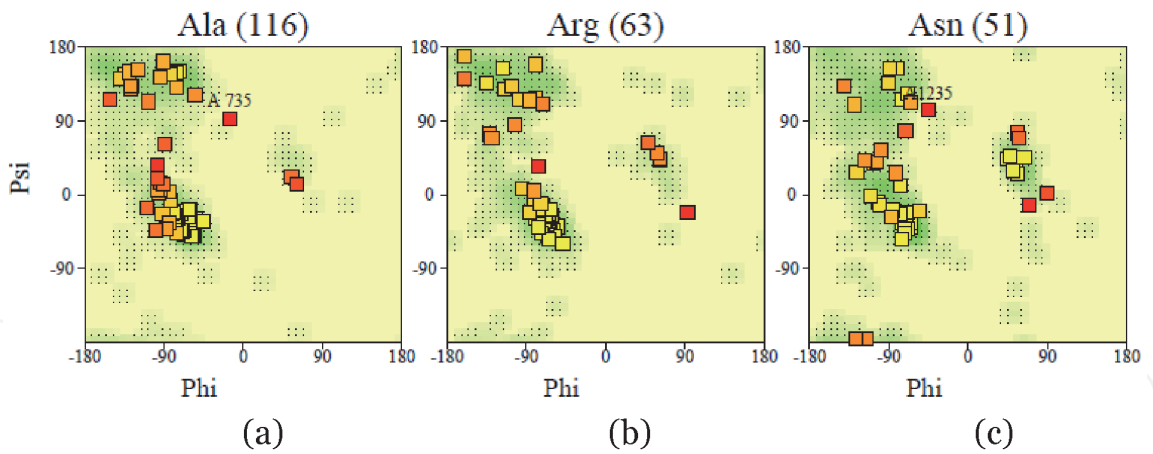
Figure 6.
Phi-psi plot of residues of the P-glycoprotein structure of Onchocerca volvulus, *modeled using the 4F4C template (a) Ala, (b) Arg, and (c) Asn.*

Rank of complex	Free binding energy (kcal/mol)
1	−5.00
2	−4.84
3	−4.2
4	−4.41
5	−3.77
6	−3.48
7	−2.96
8	−2.64
9	−2.54
10	−2.48

Table 7.
*Interaction of the drug benznidazole with P-glycoprotein (*Leishmania major*).*
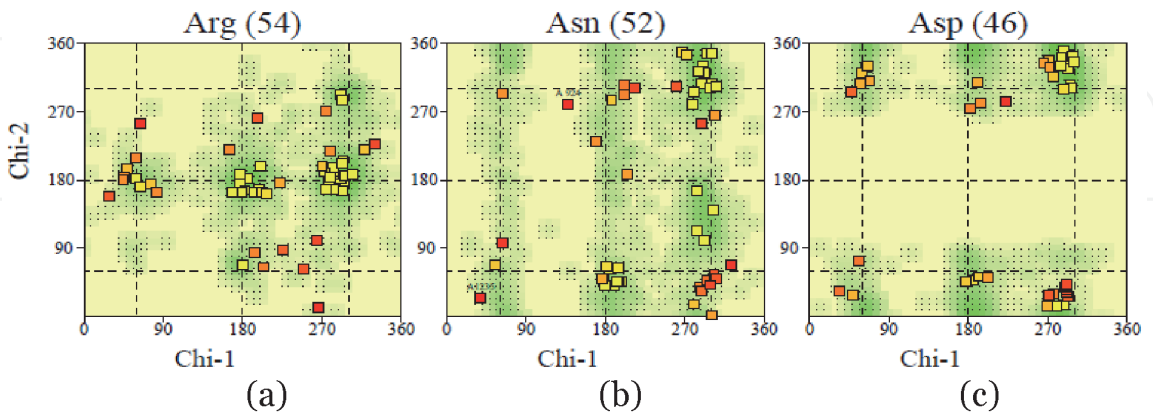
Figure 7.
Chi1-Chi2 plot of residues of the P-glycoprotein structure of Onchocerca volvulus, *modeled using the 4F4C template. (a) Arg, (b) Asn, and (c) Asp.*

clustering is at −5.66 kcal/mol. This shows that convergence to the best pose can be achieved through consecutive dockings with more iterations. **Figure 8(b)** depicts the binding site on the receptor, and **Figure 8(c)** shows the interacting residues in the benznidazole-P-glycoprotein (*Leishmania major*) docked complex viewed through RasMol 2.1.

Figure 8.
(a) Clustering analysis of the benznidazole- P-glycoprotein docked complex. (b) Location of the binding site on the receptor (P-glycoprotein [Leishmania major]). (c) The interacting residues in the benznidazole-P-glycoprotein (Leishmania major) docked complex is viewed using RasMol 2.1.

Rank of complex	Free binding energy (kcal/mol)
1	−5.29
2	−5.01
3	−4.78
4	−5.14
5	−5.08
6	−5.02
7	−4.59
8	−4.53
9	−4.42
10	34.78

Table 8.
Interaction of the drug niclosamide with P-glycoprotein (Onchocerca volvulus).

Figure 9.
(a) Clustering analysis of the niclosamide- P-glycoprotein docked complex. (b) Location of the binding site on the receptor (P-glycoprotein [Onchocerca volvulus]). (c) The interacting residues in the niclosamide- P-glycoprotein (Onchocerca volvulus) docked complex is viewed using RasMol 2.1.

Rank of complex	Free binding energy (kcal/mol)
1	−5.83
2	−5.51
3	−5.21
4	−4.71
5	−4.47
6	−4.15
7	−3.57
8	9.34
9	29.83
10	36.47

Table 9.
*Interaction of the drug Praziquantel with P-glycoprotein (*Schistosoma mansoni*).*

Figure 10.
*(a) Clustering analysis of the Praziquantel-P-glycoprotein docked complex. (b) Location of the binding site on the receptor (P-glycoprotein [*Schistosoma mansoni*]). (c) The interacting residues in the Praziquantel-P-glycoprotein [*Schistosoma mansoni*] docked complex are viewed using RasMol 2.1.*

Rank of complex	Free binding energy (kcal/mol)
1	−6.23
2	−6.04
3	−5.67
4	−4.81
5	−5.92
6	−5.25
7	−4.89
8	−4.83
9	−4.15
10	−3.34

Table 10.
*Interaction of the drug cladosporin with P-glycoprotein (*Trypanosoma cruzi*).*

3.6.2 Molecular docking results of niclosamide with P-glycoprotein
    *(*Onchocerca volvulus*)*

The best pose has a free binding energy of −5.29 kcal/mol (**Table 8**). The clustering figure shows the most number of conformations at −1.30 kcal/mol (**Figure 9**). **Figure 9(b)** depicts the binding site on the receptor, and **Figure 9(c)** shows the interacting residues in the niclosamide-P-glycoprotein (*Onchocerca volvulus*) docked complex viewed through RasMol 2.1.

3.6.3 Molecular docking results of praziquantel with P-glycoprotein
    *(*Schistosoma mansoni*)*

The best pose has a free binding energy of −5.83 kcal/mol (**Table 9**). The clustering figure (**Figure 10**) shows the most number of conformations at −5.0 kcal/mol. **Figure 10(b)** depicts the binding site on the receptor, and **Figure 10(c)** shows the interacting residues in the Praziquantel-P-glycoprotein (*Schistosoma mansoni*) docked complex viewed through RasMol 2.1.

3.6.4 Molecular docking results of cladosporin with P-glycoprotein
    *(*Trypanosoma cruzi*)*

The best pose has a free binding energy of −6.23 kcal/mol (**Table 10**). The clustering figure (**Figure 11**) shows the most number of conformations at −5.0 kcal/mol. **Figure 11(b)** depicts the binding site on the receptor, and **Figure 11(c)** shows the interacting residues in the the cladosporin-P-glycoprotein (*Trypanosoma cruzi*) docked complex viewed through RasMol 2.1.

These steps were carried out for each receptor-ligand complex, and the least free binding energy of each docked complex was determined. These results are summarized in **Table 11**.

3.7 Calculation of differential ligand binding affinity

The differential affinity of the potential drug for a given efflux pump protein relative to the known drug is estimated as the difference between the binding energies of the known and potential drugs.
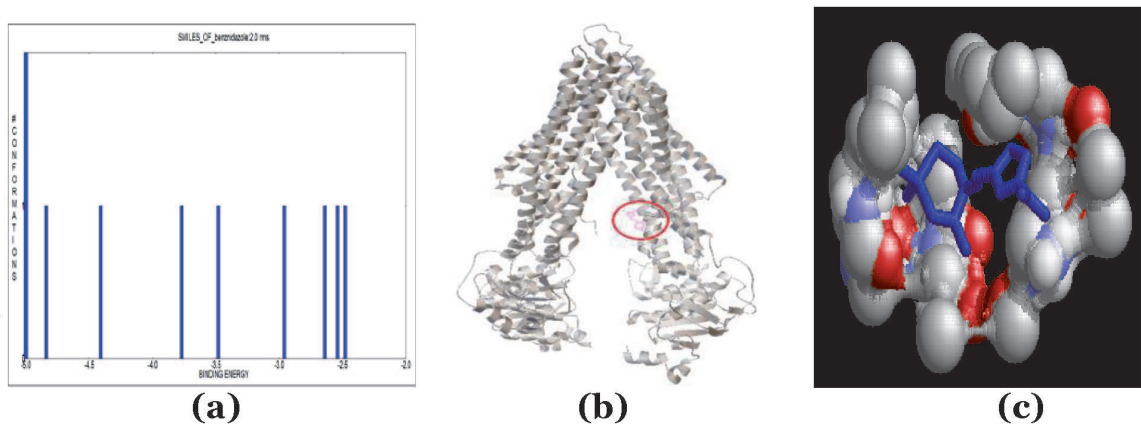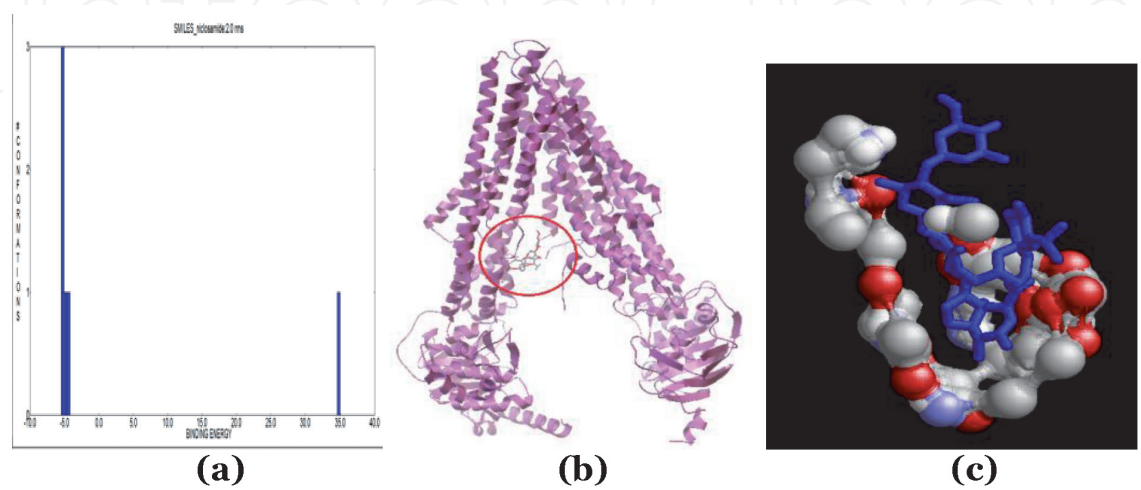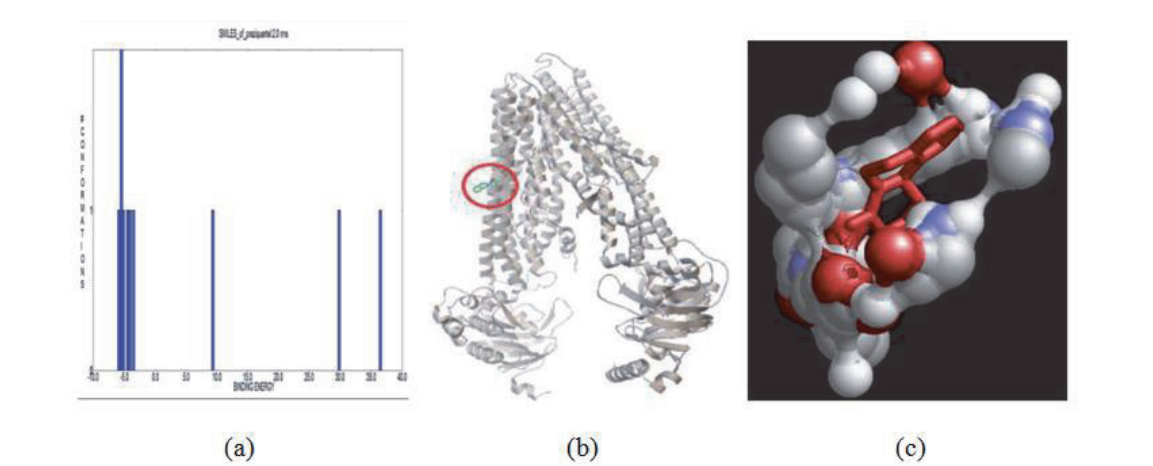

| (a) | (b) | (c) |
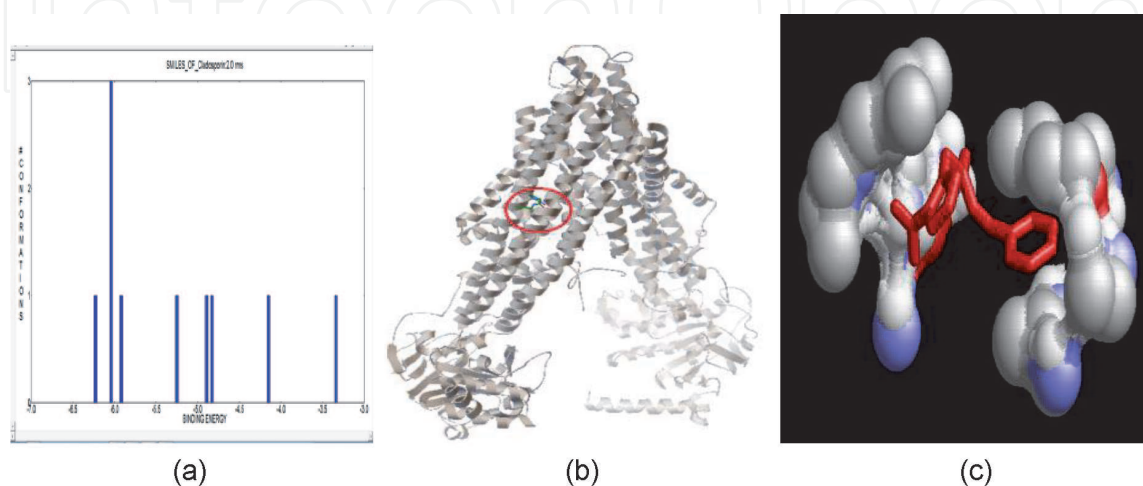
Figure 11.
*(a) Clustering analysis of the cladosporin-P-glycoprotein docked complex. (b) Location of the binding site on the receptor (P-glycoprotein [*Trypanosoma cruzi*]). (c) The interacting residues in the cladosporin-P-glycoprotein [*Trypanosoma cruzi*] docked complex are viewed using RasMol 2.1.*

	Known drugs	Free binding energy	Investigational drugs	Free binding energy
L. major	Amphotericin B	−6.44	Cladosporin	−6.42
	Fluconazole	−3.12	Jaspamide	−5.98
	Pentamidine	−2.67	Nifurtimox	−5.66
	Miltefosine	1.21	Praziquantel	−5.59
			Dapsone	−5.48
			Benznidazole	−5
			Tipifarnib	−4.54
			Flubendazole	−4.36
			Terbinafine	−4.25
			Sodium stibogluconate	−3.7
			Paromomycin	−3.07
			Meglumine antimoniate	
T. cruzi	Nifurtimox	−5.22	Cladosporin	−6.23
	Benznidazole	−5.02	Tipifarnib	−5.87
			Jaspamide	−5.82
			Fexinidazole	−4.62
			Suramin	−4.25
			Ravuconazole	−3.69
			Posaconazole	−2.52
			AN2690	
O. volvulus	Mebendazole	−5.36	Praziquantel	−6.16
	Albendazole	−5.22	Moxidectin	−5.53
	Suramin	−4.79	Niclosamide	−5.29
	Diethylcarbamazine	−3.76	Flubendazole	−4.58
	Ivermectin	−1.35	Thiabendazole	−4.35
			Metrifonate	−2.09
			Emodepside	−1.92
S. mansoni	Praziquantel	−5.83	Cladosporin	−6.07
	Mebendazole	−5.1	Jaspamide	−6.06
	Oxamniquine	−4.4	Niclosamide	−5.72
	Albendazole	−3.83	Nifurtimox	−5.62
			Artesunate	−5.12
			Benznidazole	−4.41
			Tipifarnib	−4.38
			Imatinib	−4.29
			Furozan	−4.27
			Suramin	−3.85
			Metrifonate	−3.54

Table 11.
Free binding energy of all known and investigational drugs, including repurposed antibiotics.

Leishmaniasis	ΔG unknown	ΔΔG amphotericin B	ΔΔG fluconazole	ΔΔG pentamidine	ΔΔG miltefosine
Cladosporin	−6.42	0.02	−3.3	−3.75	−7.63
Jaspamide	−5.98	0.46	−2.86	−3.31	−7.19
Nifurtimox	−5.66	0.78	−2.54	−2.99	−6.87
Praziquantel	−5.59	0.85	−2.47	−2.92	−6.8
Dapsone	−5.48	0.96	−2.36	−2.81	−6.69
Benznidazole	−5	1.44	−1.88	−2.33	−6.21
Tipifarnib	−4.54	1.9	−1.42	−1.87	−5.75
Flubendazole	−4.36	2.08	−1.24	−1.69	−5.57
Terbinafine	−4.25	2.19	−1.13	−1.58	−5.46
Sodium stibogluconate	−3.7	2.74	−0.58	−1.03	−4.91
Paromomycin	−3.07	3.37	0.05	−0.4	−4.28

Trypanosomiasis	ΔG unknown	ΔΔG Benznidazole	ΔΔG Nifurtimox
Cladosporin	−6.23	−1.21	−1.01
Tipifarnib	−5.87	−0.85	−0.65
Jaspamide	−5.82	−0.8	−0.6
Fexinidazole	−4.62	0.4	0.6
Suramin	−4.25	0.77	0.97
Ravuconazole	−3.69	1.33	1.53
Posaconazole	−2.52	2.5	2.7

Onchocerciasis	ΔG unknown	ΔΔG Mebendazole	ΔΔG Albendazole	ΔΔG Suramin	ΔΔG Diethylcarbamazine	ΔΔG Ivermectin
Praziquantel	−6.16	−0.8	−0.94	−1.37	−2.4	−4.81
Moxidectin	−5.53	−0.17	−0.31	−0.74	−1.77	−4.18
Niclosamide	−5.29	0.07	−0.07	−0.5	−1.53	−3.94
Flubendazole	−4.58	0.78	0.64	0.21	−0.82	−3.23
Thiabendazole	−4.35	1.01	0.87	0.44	−0.59	−3
Metrifonate	−2.09	3.27	3.13	2.7	1.67	−0.74
Emodepside	−1.92	3.44	3.3	2.87	1.84	−0.57

Schistosomiasis	ΔG unknown	ΔΔG Praziquantel	ΔΔG Mebendazole	ΔΔG Oxamniquine	ΔΔG Albendazole
Cladosporin	−6.07	−0.24	−0.97	−1.67	−2.24
Jaspamide	−6.06	−0.23	−0.96	−1.66	−2.23
Niclosamide	−5.72	0.11	−0.62	−1.32	−1.89
Nifurtimox	−5.62	0.21	−0.52	−1.22	−1.79
Artesunate	−5.12	0.71	−0.02	−0.72	−1.29
Benznidazole	−4.41	1.42	0.69	−0.01	−0.58
Tipifarnib	−4.38	1.45	0.72	0.02	−0.55
Imatinib	−4.29	1.54	0.81	0.11	−0.46
Furozan	−4.27	1.56	0.83	0.13	−0.44
Suramin	−3.85	1.98	1.25	0.55	−0.02
Metrifonate	−3.54	2.29	1.56	0.86	0.29

Table 12.
Differential ligand binding affinity for each known-potential drug pair.

$$\Delta\Delta G_{\text{invest.}} = \Delta G_{\text{bind,potential}} - \Delta G_{\text{bind,known}}$$

where $\Delta\Delta G_{\text{invest.}}$ = differential ligand affinity, kcal/mol; ΔG_{bind} = free energy of binding, kcal/mol.

For each disease, the differential ligand binding affinity is calculated for every known-potential drug pair. The $\Delta\Delta G_{\text{investiational}}$ values are given in **Table 12**. All values are expressed in kcal/mol. The drugs having $\Delta\Delta G_{\text{invest}}$ values greater than the $\Delta G_{\text{invest.}}$ values may have better antihelminthic activity.

All values are expressed in kcal/mol. It can be inferred from these results that many of the repurposed antiparasitic drugs show promise for treatment against other helminths. The results shown in **Table 12** serve as an indicator of which drugs may be promising antihelminthics:

1. Leishmaniasis: Cladosporin (-7.63 kcal/mol), Jaspamide (-7.19 kcal/mol), and Nifurtimox (-6.87 kcal/mol).

2. Trypanosomiasis: Cladosporin (-1.21 kcal/mol) and Tipifarnib (-0.85 kcal/mol)

Receptor	Drug	Interacting residues
4M1M	Amphotericin B	Thr172, Asp173, Ser176, Ala683, Asp687, Ser876, Ala879, Leu880, Lys883, Lys884, Glu887, Lys996
	Fluconazole	Val129, Cys133, Ala136, Asn179, Glu180, Gly181, Gly183, Asp184, Lys185, Met188, Leu875, Asp882, Lys930, Phe934
	Pentamidine	Glu239, Leu240, Ala242, Tyr243, Ala244, Gly247, Ala248, Glu251, Arg785, Thr811, Ala815, Asn816, Ala819, Gln820
	Miltefosine	Asp173, Ser176, Lys177, Glu180, Lys185, Leu875, Ala879, Leu880, Lys883
	Cladosporin	Gln434, Leu437,Leu439, Val468, Ser470, Glu472, Val474,Asn899, Arg901, Thr902, Ser905
	Jaspamide	Leu254, Ala255, Ala256, Ile257,Arg258, Thr259,Phe800, Asn805, Thr806, Thr807, Gly808, Leu810, Glu1115, Ile1117
	Nifurtimox	Ala288, Asn292, Gln769, Gly770, Phe773, Gly774, Glu778, Ala819, Gln820, Lys822, Gly823, Ser827, Phe990, Pro992
	Praziquantel	Leu254, Ala255, Ala256, Ile257,Arg258, Thr259, Phe800, Asn805, Thr806, Thr807, Leu810, Ser1113
	Dapsone	Val474, Leu475, Phe476, Ala477, Gly521, Glu522, Lys523, Lys891, Thr894, Glu895, Glu898, Asn899, His1003, Arg1006, Ile1007, Lys1010
	Benznidazole	Asp685, Val688, Pro689, Trp799, Asp802, Lys804, Asn805, Arg813, His1003, Arg1006, Ile1007, Lys1010
	Tipifarnib	Ala244, Gly247, Ala248, Val249, Glu251, Glu252, Asp1120, Gly1166, Asp1167, Lys1168
	Flubendazole	Phe159, Asp160, His162, Asp163, Val164, Ser470, Glu472, Val474, Ile897, Gly898, Asn899, Phe900, Arg901, Thr902
	Terbinafine	Phe159, Val164, Gln434, Gln437, Leu439, Val468, Ser470, Glu472, Val474, Ile897, Glu898, Asn899, Phe900, Arg901, Thr902, Ser905
	Sodium stibogluconate	Ser470, Glu472, Pro473, Val474, Leu475, Ala477, Glu522, Lys532, Glu895, Glu898, Asn899, Arg901, Thr902
	Paromomycin	Val164, Glu472, Pro473, Val474, Glu522, Glu898, Asn899

Table 13.
Interacting residues between the P-glycoprotein of Leishmania major *and the chosen drugs.*

Receptor	Drug	Interacting residues
4F4C	Mebendazole	Glu267, Thr268, Tyr271, Ala272, Gly275, Lys276, Lys315, Arg830, Ala860, Thr861, Pro864, Arg867
	Albendazole	Glu36, Gly37, Asp38, Ile40, Glu267, Thr268, Tyr271, Val305, Ala308, Lys309, Glu823, Thr826, Arg827, Arg830, Ala860, Thr861, Pro864, Arg867
	Suramin	Lys720, Leu723, Ser724, Lys727, Lys923, Val925, Lys936
	Diethylcarbamazine	Arg918, Arg919, Phe920, Gly922, Lys923, Asn924, Gln979
	Ivermectin	Arg172, Thr197, Phe200, Asp201, Glu204, Lys720, Lys923, Asn924, Val925, Ala928, Phe931, Ala932, Gly935, Lys936, Ile939
	Praziquantel	Leu11, Glu165, Lys207, Asp212, Arg918, Phe920, Lys923, Asn924, Ser927, Phe931, Ala972, Glu975, Gln979
	Moxidectin	Leu11, Arg12, Asp15, Lys26, Lys30, Glu33, Pro374, Gln913, Tyr914, Arg916, Gly917, Gly1032, Phe1033, Thr1035, Ser1036, Pro1039
	Niclosamide	Asn4, Gly5, Ser6, Leu7, Ile48, Thr49, Val56, Lys59, Gly380, Thr381, Gln383, Gly384
	Flubendazole	Glu36, Gly37, Ser42, Thr268, Tyr271, Ala272, Gly275, Arg830, Ala860, Thr861, Pro864, Asn865, Arg867, Lys1043
	Thiabendazole	Phe504, Asn505, Cys506, Asp933, Lys936, Ile937, Glu940, Phe957, Asn960, Lys964
	Metrifonate	Gln840, His841, Gly843, Phe844, Ser847, Gln849, Asn850, Lys1057, Ile1058, Lys1060
	Emodepside	Arg172, Thr197, Phe200, Asp201, Glu204, Asp550, Val925, Ser929, Phe931, Ala932, Gly935, Lys936, Ile939

Table 14.
Interacting residues between the P-glycoprotein of Onchocerca volvulus *and the chosen drugs.*

Receptor	Drug	Interacting residues
4F4C	Nifurtimox	Asn733, Asn734, Gln849, Asn850, Arg1056, Lys1057, Ile1058
	Benznidazole	Asn4, Gly5, Ser6, Leu7, Thr49, Glu55, Val56, Arg205,Thr381,Gly384, Ala385
	Cladosporin	Tyr35, Glu36, Ile40, Glu267, Thr268, Tyr271, Ala272, Gly275, Lys315, Arg830, Ala860, Thr861, Arg867
	Tipifarnib	Gly373, Asp38, Ile40, Asp41, Ser42, Asn43, Glu267, Thr268, Tyr271, Ala272, Gly275, Arg830, Ser856, Thr857, Ala860, Thr861, Arg867
	Jaspamide	Gln913, Tyr914, Arg916, Gly917, Arg918, Arg919, Lys923, Gly1032, Ph1033, Thr1035, Ser1036, Phe1038, pro1039
	Fexinidazole	Gly37, Asp38, Ile40, Asp41, Ser42, Asn43, Thr268, Tyr271, Ala272, Gly275, Arg830, Ser856, Ala860, Thr861, Pro864, Arg867
	Suramin	,Lys727, Lys923, Val925
	Ravuconazole	Ala910, Gln913, Tyr914, Gly917, Arg919, Gly1032, Phe1033, Thr1035, Ser1036, Pro1039
	Posaconazole	Glu33, Leu161, Gly917, Arg918, Arg919, Phe920, Gly922, Lys923, Asn924, Glu975, Ala976, Gln979, Phe1033, Thr1035, Ser1036, Pro1039

Table 15.
Interacting residues between the P-glycoprotein of Schistosoma mansoni *and the chosen drugs.*

3. Schistosomiasis: Cladosporin (−2.24 kcal/mol) and Jaspamide (−2.23 kcal/mol)

4. Onchocerciasis: Praziquantel (−4.81 kcal/mol) and Moxidectin (−4.18 kcal/mol)

3.8 Analysis of interacting residues in each docked complex

The best pose of each docked complex was viewed using RasMol 2.1, and all interacting residues within a radius of 4.5 Å of the ligand were restricted and analyzed. The results are summarized in **Tables 13–16**.

The interacting residues are shown and the binding pockets found in each protein sequence with respect to different drugs are highlighted. Analysis of the interacting residues showed certain binding pockets in each efflux pump protein studied. Certain residues were found to be preferred over others, for drug binding. These preferred binding pockets are:

Receptor	Drug	Interacting residues
4F4C	Praziquantel	Asn505, Arg551, Asp933, Lys936, Ile937, Ile939, Glu940, Glu943, Asn944, Lys964
	Mebendazole	Arg172, Thr197, Phe200, Asp201, Glu204, Lys207, Asn924, Ala928, Phe931, Ala932, Gly935, Ile939
	Oxamniquine	Ile40, Asp41, Ser42, Thr268, Tyr271, Ala272, Gly275, Arg830, Ser856, Ala860, Pro864, Arg867
	Albendazole	Ser42, Glu267, Thr268, Tyr271, Ala272, Gly275, Lys276, Lys315, Arg830, Ala860, Arg867
	Cladosporin	Tyr35, Glu36, Gly37, Ile40, Phe263, Ala264, Ile265, Glu267, Thr268, Tyr271, Lys315, Arg830, Thr861, Asn865, Arg867, Thr868, Glu1040, Lys1043
	Jaspamide	Leu161, Lys207, Glu208, Gly211, Asp212, Lys213, Gly917, Arg918, Arg919, Phe920, Gly922, Lys923, Asn924, Gln979
	Niclosamide	Lys26 Lys30, Ala910, Gln913, Tyr914, Arg916, Gly917, Leu1031, Gly1032, Phe1033, Thr1035
	Nifurtimox	Tyr35, Glu36, Gly37, Ile40, Phe263, Ala264, Glu267, Thr268, Lys315, Pro864, Asn865, Arg867, Thr868, Glu1040, Lys1043
	Artesunate	Arg8, Leu11, Arg12, Asp15, Lys26, Lys30, Leu371, Pro374, Arg916, Phe1033, Thr1035
	Benznidazole	Asn505, Arg551, Asp933, Lys936, Ile937, Glu940, Lys964
	Tipifarnib	Leu161, Glu204, Lys207, Glu208, Gly211, Asp212, Lys213, Val378, Asn924
	Imatinib	Ser42, Asn43, Glu267, Tr268, Tyr271, Ala272, Gly275, Lys276, Arg830, Ala860, Thr861, Arg867,
	Furozan	Ala910, Gln913, Tyr914, Arg916, Gly917, Arg919, Lys923, Gly1032, Thr1035, Ser1036, Phe1038, Pro1039
	Suramin	Asn4, Arg8, Asp51, Glu55, Thr194, Asp201, Asn202, Arg205, Glu716, Gly719, Lys720, Asp721
	Metrifonate	Ile40, Phe263, Ala264, Glu267, Thr268, Tyr271, Ala308, Lys315, Arg830, Ala860, Pro864, Arg867

Table 16.
Interacting residues between the P-glycoprotein of Trypanosoma cruzi *and the chosen drugs.*

1. P-glycoprotein (*Leishmania major*): **(Ser470, Glu472, Val474, Ile897, Glu898, Asn899, Phe900, Arg901, Thr902, Ser905)**

2. P-glycoprotein (*Onchocerca volvulus*): **(Arg830, Ala860, Thr861, Pro864, Arg867)**

3. P-glycoprotein (*Schistosoma mansoni*): **(Glu267, Thr268, Tyr271, Ala272, Gly275, Lys276)**

4. P-glycoprotein (*Trypanosoma cruzi*): **(Arg830, Ala860, Thr861, Arg867); (Gly917, Arg918, Arg919, Phe920, Gly922, Lys923); (Phe1033, Thr1035, Ser1036, Pro1039)**

3.9 P-glycoprotein in *E. coli*

A PSI-BLAST was performed to search for P-glycoprotein homologs in *E. coli* using hPGP as the query. The top BLAST hits showed low percentage identity (< 30%) and low score and were not annotated as bacterial P-glycoprotein. Though we could not reliably ascertain P-glycoprotein homologs in *E. coli*, there exist other mechanisms that could potentially lead to multidrug resistance phenotypes in *E. coli*. Multidrug efflux systems are of five types, namely the super-families ATP Binding Cassete (ABC) and Major Facilitador Super-family (MFS), Small Multidrug Resistance (SMR), Resistance, Nodulation, Division (RND) and Multidrug and Toxic Compound Extrusion (MATE). In *E.coli*, the examples for various systems include: MFS system Bcr, EmrB and EmrD; SMR family EmrE; RND family AcrB; and Mate family YdhE9 [39]. *E. coli* contains five putative ABC-type MDR-like transporters. These systems were all cloned and expressed in a drug-sensitive *E. coli* strain, and the drug resistance phenotypes were investigated. None of these systems provided an appreciable drug resistance to *E. coli*, except for YbjYZ, which conferred resistance to erythromycin [40]. The AcrAB-TolC system of *E. coli* is one of the best-characterized MDR transporters that is responsible for the acquisition of multiple antimicrobial resistance of the *mar* mutants, including resistance to tetracycline, chloramphenicol, ampicillin, nalidixic, and rifampicin [41, 42]. *E. coli* infections could modulate the pharmacokinetics of the drug enrofloxacin by altering the expression of intestinal P-glycoprotein in broilers [43].

4. Conclusions

The study of the human P-glycoprotein homologs, namely the P-glycoproteins of *Leishmania major*, *Onchocerca volvulus*, *Schistosoma mansoni*, and *Trypanosoma cruzi* has provided an insight into their drug resistance mechanisms. The investigational drugs such as cladosporin, jaspamide, nifurtimox, and tipifarnib are strong contenders for novel antihelminthic treatment. Known drugs such as praziquantel and moxidectin have shown great promise for use as treatment against other helminthic diseases.

Author details

Nivedita Jaishankar[1], Sangeetha Muthamilselvan[2] and Ashok Palaniappan[2*]

1 Department of Biotechnology, Sri Venkateswara College of Engineering, Sriperumbudur, India

2 Department of Bioinformatics, School of Chemical and BioTechnology, SASTRA Deemed University, Thanjavur, India

*Address all correspondence to: apalania@scbt.sastra.edu

IntechOpen

References

[1] Nikaido H. Multidrug resistance in bacteria. Annual Review of Biochemistry. 2009;**78**:119-146. DOI: 10.1146/annurev.biochem.78.082907. 145923

[2] Handzlik J, Matys A, Kieć-Kononowicz K. Recent advances in multi-drug resistance (MDR) efflux pump inhibitors of gram-positive bacteria S. aureus. Antibiotics. 2013;**2**(1):28-45. DOI: 10.3390/ antibiotics2010028

[3] Sharma A, Gupta VK, Pathania R. Efflux pump inhibitors for bacterial pathogens: From bench to bedside. The Indian Journal of Medical Research. 2019;**149**(2):129-145. DOI: 10.4103/ ijmr.IJMR_2079_17

[4] Higgins CF, Callaghan R, Linton KJ, Rosenberg MF, Ford RC. Seminars in cancer biology. Structure of the multidrug resistance P-glycoprotein. 1997;**8**:135-142

[5] Amin ML. P-glycoprotein inhibition for optimal drug delivery. Drug Target Insights. 2013;7:27-34. DOI: 10.4137/ DTI.S12519

[6] Jin MS, Oldham ML, Zhang Q, Chen J. Crystal structure of the multidrug transporter P-glycoprotein from *C. elegans*. Nature. 2012; **490**(7421):566-569. DOI: 10.1038/ nature11448

[7] Sauna ZE, Muller MM, Kerr KM, Ambudkar SV. The mechanism of action of multidrug-resistance- linked P-glycoprotein. Journal of Bioenergetics and Biomembranes. 2001;**33**(6): 481-491. DOI: 10.1023/A: 1012875105006

[8] Fortuna A, ALves G, Falcao A. In vitro and in vivo relevance of the P-glycorotein probe substrates in drug discovery and development: Focus on rhodamine 123, digoxin and talinolol. Journal of Bioequivalence and Bioavailablity. 2012;**01**(02):22. DOI: 10.4172/jbb.S2-001

[9] Sheps JA, Ralph S, Zhao Z, et al. The ABC transporter gene family of *Caenorhabditis elegans* has implications for the evolutionary dynamics of multidrug resistance in eukaryotes. Genome Genome Biology. 2004;**5**:R15. DOI: 10.1186/gb-2004-5-3-r15

[10] Laing N, Speicher LA, Smith CD, Tew KD. P-glycoprotein binding and modulation of the multidrug resistance phenotype by Estramustine. Journal of the National Cancer Institute. 1994; **86**(9):688-694. DOI: 10.1093/jnci/ 86.9.688

[11] Bourguinat C, Ardelli BF, Pion SDS, Kamgno J, Gardon J, Duke BOL, et al. P-glycoprotein-like protein, a possible genetic marker for ivermectin resistance selection in *Onchocerca volvulus*. Molecular and Biochemical Parasitology. 2008;**158**(2):101-111. DOI: 10.1016/j. molbiopara.2007.11.017

[12] Gamarro F, Chiquero MJ, Amador MV, Castanys S. P-glycoprotein overexpression in methotrexate-resistant *Leishmania*. Biochemical Pharmacology. 1994;**47**(11):1939-1947. DOI: 10.1016/0006-2952(94)90067-1

[13] Piscopo TV, Mallia AC. Leishmaniasis. Postgraduate Medical Journal. 2007;**83**(976):649-657. DOI: 10.1136/pgmj.2006.047340corr1

[14] Barrett MP, Croft SL. Management of trypanosomiasis and leishmaniasis. British Medical Bulletin. 2012;**104**: 175-196. DOI: 10.1093/bmb/lds031

[15] Wyllie S, Cunningham ML, Fairlamb AH. Dual action of antimonial drugs on thiol redox metabolism in the human pathogen *Leishmania donovani*.

The Journal of Biological Chemistry. 2004;**279**(38):39925-39932. DOI: 10.1074/jbc.M405635200

[16] Soares ROA, Echevarria A, Bellieny MSS, Pinho RT, de Leo RMM, Seguins WS, et al. Evaluation of thiosemicarbazones and semicarbazones as potential agents anti-*Trypanosoma cruzi*. Experimental Parasitology. 2011;**129**(4):381-387. DOI: 110.1016/j. exppara.2011.08.019

[17] de Silva NR, Brooker S, Hotez PJ, Montresor A, Engels D, Savioli L. Soil-transmitted helminth infections: Updating the global picture. Trends in Parasitology. 2003;**19**(12):547-551. DOI: 10.1016/j.pt.2003.10.002

[18] Colley DG, Bustinduy AL, Secor WE, King CH. Human schistosomiasis. Lancet. 2014;**383**(9936):2253-2264. DOI: 10.1016/S0140-6736(13)61949-2

[19] Pinto-Almeida A, Mendes T, Armada A, et al. The role of efflux pumps in *Schistosoma mansoni* Praziquantel resistant phenotype. PLoS One. 2015;**10**(10):e0140147. DOI: 10.1371/journal.pone.0140147

[20] Cobo F. 10—Trypanosomiasis. In: Cobo F, editor. Imported Infectious Diseases. Cambridge: Woodhead Publishing; 2014. pp. 137-153. ISBN: 9781907568572. DOI: 10.1533/9781908818737.137

[21] Maya JD, Cassels BK, Iturriaga-Vásquez P. Mode of action of natural and synthetic drugs against *Trypanosoma cruzi* and their interaction with the mammalian host. Comparative Biochemistry and Physiology A Molecular and Integrative Physiology. 2007;**146**(4):601-620. DOI: 10.1016/j. cbpa.2006.03.004

[22] Bahia MT, de Andrade IM, Martins TA, et al. Fexinidazole: A potential new drug candidate for Chagas disease. PLoS Neglected Tropical Diseases. 2012;**6**(11):e1870. DOI: 10.1371/journal.pntd.0001870

[23] Liu J, Hajibeigi A, Ren G, Lin M, Siyambalapitiyage W, Liu Z, et al. Retention of the radiotracers 64Cu-ATSM and 64Cu-PTSM in human and murine tumors is influenced by MDR1 protein expression. Journal of Nuclear Medicine. 2009;**50**(8):1332-1339. DOI: 10.2967/jnumed.109.061879

[24] Rappa G, Lorico A, Liu MC, Kruh GD, Cory AH, Cory JG, et al. Overexpression of the multidrug resistance genes mdr1, mdr3 and mrp in L1210 leukemia cells resistant to inhibitors of ribonucleotide reductase. Biochemical Pharmacology. 1997;**54**: 649-655. DOI: 10.1016/s0006-2952(97)00210-4

[25] Campos MCO, Castro-Pinto DB, Ribeiro GA, Berredo-Pinho MM, Gomes LHF, Bellieny MS, et al. P-glycoprotein efflux pump plays an important role in *Trypanosoma cruzi* drug resistance. Parasitology Research. 2010;**112**:2341-2351. DOI: 10.1007/s00436-010-1988-6

[26] Kumar A, Muthamilselvan S, Palaniappan A. Computational studies of drug repurposing targeting P-glycoprotein-mediated multidrug resistance phenotypes in priority infectious agents. In: Creatinine—a Comprehensive Update. Rijeka: Intechopen; 2020. DOI: 10.5772/intechopen.90745

[27] Bhagwat M, Aravind L. PSI-BLAST tutorial. In: Bergman NH, editor. Comparative Genomics: Volumes 1 and 2. Totowa (NJ): Humana Press; 2007. Available from: https://www.ncbi.nlm.nih.gov/books/NBK2590/.ch 10

[28] Chenna R, Sugawara H, Koike T, Lopez R, Gibson TJ, Higgins DG, et al. Multiple sequence alignment with the Clustal series of programs. Nucleic

Acids Research. 2013;**31**(13):3497-3500. DOI: 10.1093/nar/gkg500

[29] Biasini M, Bienert S, Waterhouse A, Arnold K, Studer G, Schmidt T, et al. SWISS-MODEL: Modelling protein tertiary and quaternary structure using evolutionary information. Nucleic Acids Research. 2014;**42**(Web Server Issue): W252-W258. DOI: 10.1093/nar/gku340

[30] Schwede T, Kopp J, Guex N, Peitsch MC. SWISS-MODEL: An automated protein homology-modeling server. Nucleic Acids Research. 2003;**31**(13):3381-3385. DOI: 10.1093/nar/gkg520

[31] Weininger D, Weininger A, Weininger JL. SMILES 2. Algorithm for generation of unique SMILES notation. Journal of Chemical Information and Computer Sciences. 1989;**29**(2):97-101. DOI: 10.1021/ci00062a008

[32] Morris GM, Huey R, Lindstrom W, Sanner MF, Belew RK, Goodsell DS, et al. Autodock4 and AutoDockTools4: Automated docking with selective receptor flexiblity. Journal of Computational Chemistry. 2009;**30**(16): 2785-2791. DOI: 10.1002/jcc.21256

[33] Sayle RA, Milner-White EJ. RASMOL: Biomolecular graphics for all. Trends in Biochemical Sciences. 1995; **20**(9):374. DOI: 10.1016/s0968-0004 (00)89080-5

[34] Messerli SM, Kasinathan RS, Morgan W, Spranger S, Greenberg RM. *Schistosoma mansoni* P-glycoprotein levels increase in response to praziquantel exposure and correlate with reduced praziquantel susceptibility. Molecular And Biochemical Parasitology. 2009;**167**(1): 54-59. DOI: 10.1016/j.molbiopara. 2009.04.007

[35] Buckner FS, Waters NC, Avery VM. Recent highlights in anti-protozoan drug development and resistance research. International Journal of Parasitology Drugs and Drug Resistance. 2012;**2**:230-235. DOI: 10.1016/j. ijpddr.2012.05.002

[36] García MT, Lara-Corrales I, Kovarik CL, Pope E, Arenas R. Tropical skin diseases in children: A review-part II. Pediatric Dermatology. 2016;**33**: 264-274. DOI: 10.1111/pde.12778

[37] Kappagoda S, Singh SMU, Blackburn BG. Antiparasitic therapy. Mayo Clinic Proceedings. 2011;**86**(6): 561-583. DOI: 10.4065/mcp.2011.0203

[38] Varghese S, Palaniappan A. Computational pharmacogenetics of P-glycoprotein mediated antiepileptic drug resistance. The Open Bioinformatics Journal. 2018;**11**:197-207. DOI: 10.2174/1875036201811010197

[39] Moreira MAS, de Souza EC, de Moraes CA. Multidrug efflux systems in gram-negative bacteria. Brazilian Journal of Microbiology. 2004;**35**(1):2. DOI: 10.1590/S1517-8382200400 0100003

[40] Nishino K, Yamaguchi A. Analysis of a complete library of putative drug transporter genes in *Escherichia coli*. Journal of Bacteriology. 2001;**183**: 5803-5812

[41] Ma D, Cook DN, Alberti M, Pon NG, Nikaido H, Hearst JE. Molecular cloning and characterization of acrA and acrE genes of *Escherichia coli*. Journal of Bacteriology. 1993;**175**: 6299-6313

[42] Ma D, Cook DN, Alberti M, Pon NG, Nikaido H, Hearst JE. Genes acrA and acrB encode a stress-induced efflux system of *Escherichia coli*. Molecular Microbiology. 1995;**16**:45-55

[43] Lubelski J, Konings WN, Driessen AJM. Distribution and physiology of ABC-type transporters contributing to multidrug resistance in bacteria. Microbiology and Molecular Biology Reviews. 2007;**71**(3):463-476. DOI: 10.1128/MMBR.00001-07